nature medicine

Biofilm-like extracellular viral assemblies mediate HTLV-1 cell-to-cell transmission at virological synapses

Ana-Monica Pais-Correia[1], Martin Sachse[2], Stéphanie Guadagnini[2], Valentina Robbiati[1], Rémi Lasserre[1], Antoine Gessain[3], Olivier Gout[4], Andrés Alcover[1] & Maria-Isabel Thoulouze[1]

Human T cell leukemia virus type 1 (HTLV-1) is a lymphotropic retrovirus whose cell-to-cell transmission requires cell contacts. HTLV-1–infected T lymphocytes form 'virological synapses', but the mechanism of HTLV-1 transmission remains poorly understood. We show here that HTLV-1–infected T lymphocytes transiently store viral particles as carbohydrate-rich extracellular assemblies that are held together and attached to the cell surface by virally-induced extracellular matrix components, including collagen and agrin, and cellular linker proteins, such as tetherin and galectin-3. Extracellular viral assemblies rapidly adhere to other cells upon cell contact, allowing virus spread and infection of target cells. Their removal strongly reduces the ability of HTLV-1–producing cells to infect target cells. Our findings unveil a novel virus transmission mechanism based on the generation of extracellular viral particle assemblies whose structure, composition and function resemble those of bacterial biofilms. HTLV-1 biofilm-like structures represent a major route for virus transmission from cell to cell.

HTLV-1 infects 15–20 million people worldwide[1]. Although most of the infected individuals are asymptomatic, 5–10% develop T cell leukemia or inflammatory syndromes such as HTLV-1–associated myelopathy–tropical spastic paraperesis (HAM-TSP)[1].

HTLV-1 transmission requires cell contacts[2,3]. It has previously been shown that HTLV-1–infected lymphocytes polarized their microtubules and viral components upon contact with other T cells, forming virological synapses where HTLV-1 can spread from cell to cell[4–7]. Likewise, virological synapses mediate efficient cell-to-cell transmission of HIV-1 (refs. 8,9). Hence, HTLV-1 and HIV-1 seem to hijack the T cell polarization machinery to direct virus budding to cell contacts, favoring virus transfer to target cells[4,7,9,10]. Nonetheless, the formation of 'polysynapses' by HIV-1–infected T cells indicates that stable cell polarization is not absolutely required for HIV-1 transmission[11]. Unlike T cells, dendritic cells can be infected by cell-free HTLV-1 and transmit the virus to T lymphocytes[12].

We report here that HTLV-1 cell-to-cell transmission does not necessarily occur directly through synaptic contacts. Rather, HTLV-1 virions bud at the plasma membrane and are transiently kept in adhesive extracellular structures rich in carbohydrates and composed of virally induced extracellular matrix and linker proteins that are reminiscent of bacterial biofilms[13]. These extracellular viral assemblies rapidly adhere during cell contacts to other lymphocytes supporting their infection. Our findings uncover a new and major mode of HTLV-1 cell transmission.

RESULTS

Viral components cluster on the surface of infected cells

HTLV-1–infected lymphocytes have been shown to cluster capsid (Gag) and envelope (Env) viral proteins at the cell cortex, whereas Tax viral transactivator localizes at the microtubule-organizing center and in the nucleus[4,6,14]. Upon contact with other T cells, infected cells polarize their microtubule-organizing center and Gag, Env and Tax proteins toward the cell contact. Then, viral components appear in uninfected cells, indicating that transfer of virus to target cells has occurred. This supports the notion of virological synapses as being virus-induced organized cell contacts through which HTLV-1 is transmitted from cell to cell[4,6,7]. However, the precise localization of viral components and the subcellular compartments involved have remained ill defined.

We therefore carried out confocal and electron microscopy analyses in primary $CD4^+$ T cells from HTLV-1–infected individuals and in the chronically infected cell lines C91/PL and MT2. Gag p19 has previously been shown to cluster in discrete areas of the cell cortex[4,6,14] that might be intracellular compartments where viral particles assemble, accumulate or both, ready to be transferred to target cells. To localize viral proteins with respect to the plasma membrane, we used sera reactive against various viral proteins (data not shown) from individuals with HAM-TSP, Gag p19–specific monoclonal antibody (mAb) and the lectin concanavalin-A (ConA) to label cell surface glycoproteins. To obtain maximal image definition, we performed deconvolution of confocal images and three-dimensional reconstruction.

[1]Institut Pasteur, Unité de Biologie Cellulaire des Lymphocytes, Centre National de la Recherche Scientifique (CNRS), Unité de Recherche Associée (URA) 1961, Paris, France. [2]Institut Pasteur, Plateforme de Microscopie Ultrastructurale, Imagopole, Paris, France. [3]Institut Pasteur, Unité d'Epidémiologie et Physiopathologie des Virus Oncogènes, CNRS URA 1930, Paris, France. [4]Fondation A. Rothschild, Service de Neurologie, Paris, France. Correspondence should be addressed to A.A. (andres.alcover@pasteur.fr) or M.-I.T. (marie-isabelle.thoulouze@pasteur.fr).

Received 3 August; accepted 30 October; published online 20 December 2009; doi:10.1038/nm.2065

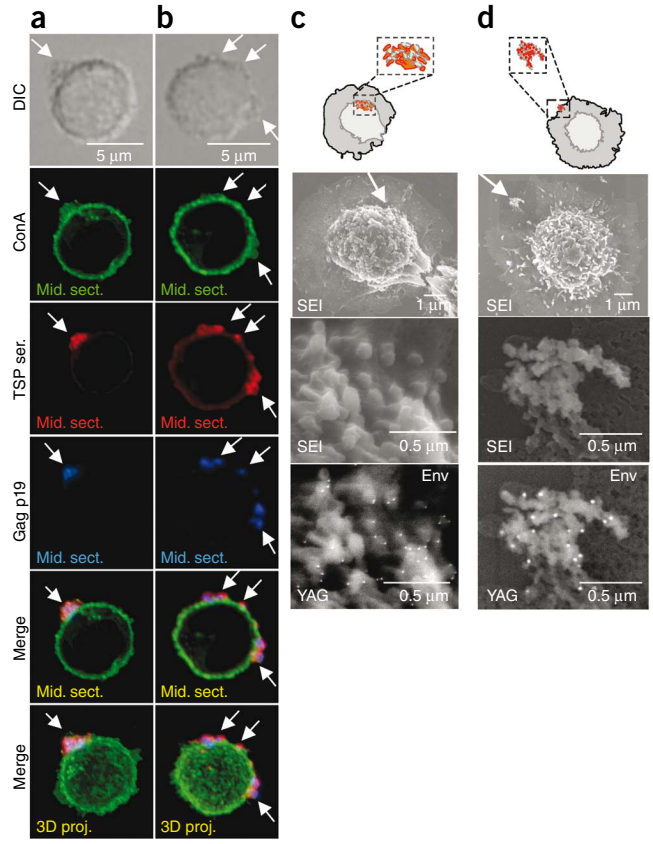

Figure 1 Clusters of viral components are on the surface of infected cells. (**a**,**b**) Confocal microscopy of primary CD4$^+$ T cells from individuals with HAM-TSP showing cell surface glycoproteins stained with Con A (green) and viral proteins stained with serum from individuals with HAM-TSP (red, TSP ser.) and with Gag p19–specific antibody (blue). Medial optical sections (Mid. sect.), or projections of three-dimensional reconstructions (3D proj.) are shown. DIC, differential interference contrast microscopy. Arrows point to viral protein clusters. Two different patterns of viral protein distribution are shown in **a** and **b**. Two different patterns of viral protein distribution are shown, a single cluster in **a** and multiple clusters in **b**. (**c**,**d**) Scanning electron microscopy of primary CD4$^+$ T cells from individuals with HAM-TSP, showing Env gp46 stained by immunogold (15 nm). Secondary electron image detection (SEI) allows visualization of cell morphology (top and middle images), whereas backscattered detection (YAG) allows gold particle detection (bottom images). Arrows point to Env$^+$ virus clusters on the cell surface (**c**) or on the edge of the membrane lamellipodium that adheres the cell to the coverslip (**d**) (top images); these areas are enlarged in the middle and bottom images. Drawings show the shape of the cell and the area showing Env$^+$ viral clusters. Data are representative of ten experiments carried out for **a** and **b** and three for **c** and **d** with cells from multiple subjects.

Strikingly, cortical clusters of viral proteins were on the cell surface, appearing as single or multiple clusters, faintly labeled by ConA (**Fig. 1a**,**b**). We found similar results in samples from all 17 subjects with HAM-TSP and two asymptomatic carriers (**Supplementary Fig. 1a** and data not shown). We did not detect viral protein clusters inside infected cells, although their plasma membrane appeared evenly and dimly stained by sera from individuals with HAM-TSP and by antibodies to Gag p19 (**Fig. 1b**). Finally, MT2 or C91/PL cells also showed viral protein clusters at the cell surface (**Supplementary Fig. 1b**,**c**). In polarized cells, we often found viral proteins on the uropod, as assessed by the enrichment in intercellular adhesion molecule-1 and phosphorylated ezrin-radixin-moesin (**Supplementary Fig. 1d**,**e**), suggesting that adhesion and cytoskeletal structures may maintain viral components polarized on the cell surface.

Viral protein clusters are extracellular viral assemblies

By scanning electron microscopy and immunogold staining of Env glycoprotein (gp46), cells from individuals with HAM-TSP showed putative Env$^+$ viral particle clusters embedded in a smooth material (**Fig. 1c**,**d**). Virus clusters were of various sizes and could be observed at the edge of membrane extensions (**Fig. 1d**). We observed similar Env$^+$ virus clusters in C91/PL and MT2 cells, but they were absent in uninfected lymphocytes (**Supplementary Fig. 2a–c**).

These data suggested that extracellular clusters of Env$^+$ viral particles are at the surface of infected cells. However, we could not rule out that Env glycoprotein shed from viral particles can concentrate in heparan sulfate proteoglycan–enriched areas[15]. We therefore performed transmission electron microscopy (**Fig. 2**). On the cell surface of MT2 cells we observed mature viral particle assemblies, showing electron-dense cores and gold labeling of Env (**Fig. 2b**) as well as empty vesicles (**Fig. 2b**). Moreover, we observed a mesh of electron-dense material among the viral particles, which may have been extracellular matrix (**Fig. 2b**). Moreover, double immunogold staining on thawed cryosections of MT2 cell pellets revealed extracellular assemblies of mature viral particles containing both Env and Gag p19 (**Fig. 2c**).

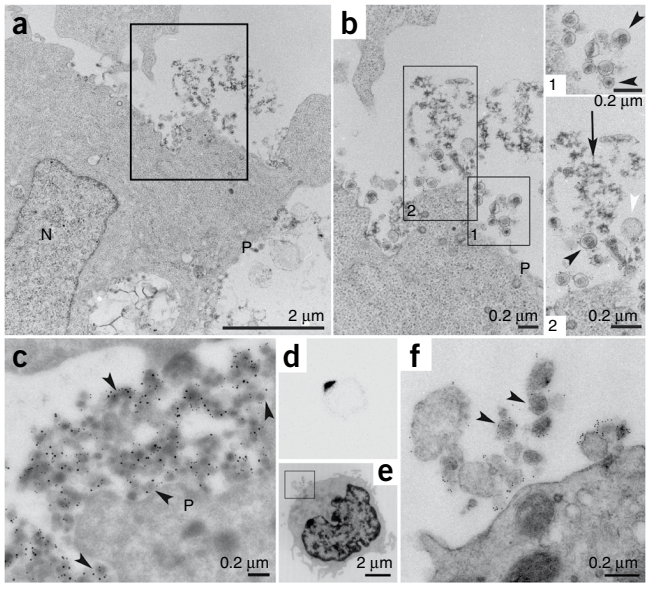

Figure 2 Extracellular viral assemblies on the surface of HTLV-1–infected cells. (**a**,**b**) Transmission electron microscopy of MT2 cells on coverslips, showing Env gp46 stained by immunogold before Epon embedding. (**b**) Enlargement of the area framed in **a**. Insets show the two framed areas marked 1 and 2. Black arrowheads show mature virus particles (dense core surrounded by an envelope labeled by gold particles). The white arrowhead shows empty vesicles lacking dense cores and gold labeling. The black arrow points to the electron-dense mesh, putatively extracellular matrix. (**c**) Cryosections of MT2 cell pellets showing immunogold staining of Env gp46 (15-nm gold) and Gag p19 (10-nm gold). P, plasma membrane. (**d**–**f**) CD4$^+$ T cells from individuals with HAM-TSP, showing Gag p19 staining by immunofluorescence and immunogold (10 nm). Infected cells identified by fluorescence microscopy (**d**) were processed for transmission electron microscopy (**e**,**f**). The framed area in **e** is enlarged in **f**. Arrowheads show mature virus particles (dense core surrounded by an envelope labeled by gold particles). Representative of five experiments performed for **a** and **b** and three for **c** and **d**–**f**.

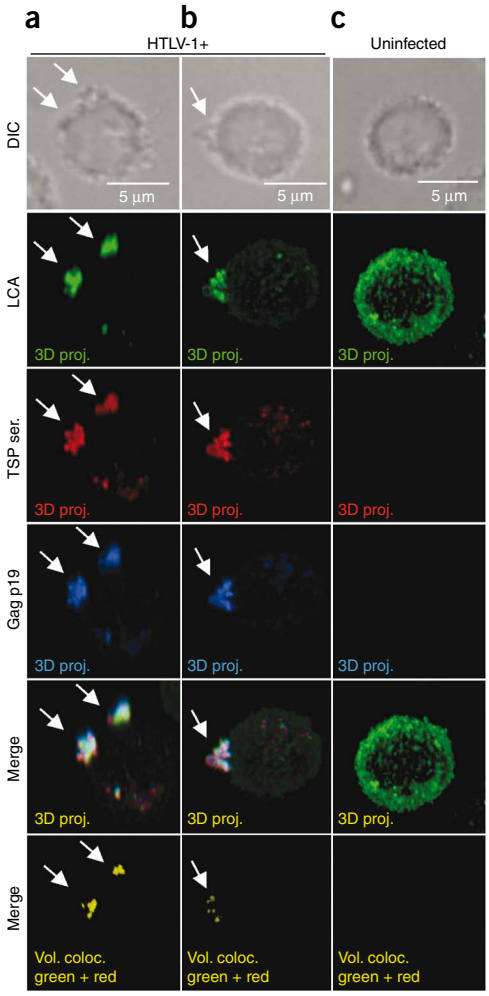

Figure 3 Extracellular HTLV-1 assemblies are carbohydrate-rich structures. Confocal microscopy of CD4$^+$ T cells from individuals with HAM-TSP, showing cell surface glycoproteins stained with LCA (green), and viral proteins stained with serum from an individual with HAM-TSP (red) and with Gag p19–specific antibody (blue). Projections of three-dimensional reconstructions are shown. Bottom images show the volume of colocalization (Vol. coloc.) of LCA and serum staining. Examples of infected (**a**,**b**) and uninfected cells (**c**) are shown. Representative of three experiments carried out with cells from two subjects.

Finally, we observed cells from individuals with HAM-TSP by correlative immunofluorescence and transmission electron microscopy (**Fig. 2d–f**). HTLV-1–positive cells by immunofluorescence (**Fig. 2d**) showed extracellular Gag p19–specific immunogold–labeled mature viral particles with membrane and dense core (**Fig. 2f**). Altogether, our light and electron microscopy observations show the presence of extracellular viral assemblies on the surface of HTLV-1–infected T lymphocytes.

Viral assemblies are carbohydrate-rich structures

Extracellular matrix components provide attachment sites for viruses, including HTLV-1, facilitating their entry[15,16]. They might also facilitate the attachment and concentration of budding viral particles into extracellular viral assemblies. To investigate this, we used plant lectins recognizing glycans enriched in the extracellular matrix[17,18] (**Supplementary Fig. 3**). We took advantage of the fact that HTLV-1 gp46 is poorly glycosylated compared with glycoproteins of many other viruses, including HIV-1 gp120 (refs. 19,20). We observed that, like ConA (**Fig. 1**), most lectins evenly stained the surface of uninfected cells (**Supplementary Fig. 3** and data not shown). However, *Lens culinaris* (LCA) and *Arachis hypogeae* (PNA) lectins strongly stained extracellular viral assemblies and evenly stained uninfected cells (**Fig. 3**). The colocalization between lectin labeling and viral markers was weak, however, indicating that lectins do not primarily bind viral Env glycoprotein but rather other glycoconjugates enriched in extracellular viral assemblies (**Fig. 3a**,**b** and **Supplementary Fig. 3a**).

Likewise, uninfected primary T cells transfected with expression vectors encoding the full-length HTLV-1 genome showed LCA labeling on viral protein clusters (**Supplementary Fig. 3b**). Finally, we observed that sialyl-LewisX (sLeX), a tetrasaccharide involved in lymphocyte adhesiveness and overexpressed upon HTLV-1 infection[21,22], was concentrated in extracellular viral assemblies (**Fig. 4a**). Thus, extracellular viral particles are embedded in a carbohydrate-rich structure that is induced and spatially reorganized by viral infection.

HTLV-1 assemblies contain extracellular matrix and linkers

We next searched for extracellular matrix components in HTLV-1 assemblies. Both collagen and fibronectin are overexpressed in HTLV-1–infected cells in a Tax-mediated manner[23,24]. We found that collagen was enriched in viral assemblies but randomly distributed on uninfected cells (**Fig. 4b**). In contrast, neither fibronectin (**Supplementary Fig. 4a**) nor laminin (data not shown) were coclustered with virions. Agrin, a heparan sulfate proteoglycan that cross-links cell surface receptors and is involved in neural, immunological and viral synapses[25–27], was also concentrated in viral clusters (**Fig. 4c** and **Supplementary Fig. 4d–f**). Notably, α-dystroglycan, a heparan sufate proteoglycan that clusters with agrin in synaptic structures[28], did not accumulate (**Supplementary Fig. 4b**), indicating preferential concentration of some proteoglycans in these structures. Finally, neuropilin, a transmembrane protein involved in HTLV-1 entry and present in HTLV-1 virological synapses[29] and immunological synapses[30], was not concentrated in extracellular viral assemblies (**Supplementary Fig. 4c**). Treatment of cells with heparinases or metalloproteinases that hydrolyze heparan sulfate proteoglycans or various extracellular matrix proteins, respectively, led to the detachment and fractionation of HTLV-1 assemblies (**Supplementary Fig. 5a–d**). This further supports the involvement of extracellular matrix in the generation of these structures.

We next hypothesized that galectins, β-galactoside–binding lectins that form lattices that condition extracellular matrix properties, could also be involved in extracellular viral assemblies. Galectin-1 and galectin-3 are secreted by T lymphocytes[31] and upregulated by HTLV-1 infection[32,33]. We found galectin-3, but not galectin-1, clustered in viral assemblies at the surface of cells from individuals with HAM-TSP (**Fig. 4d** and data not shown). However, in MT2 and C91/PL cells, galectin-3 was poorly expressed and did not cluster with viral particles (data not shown).

Finally, we found tetherin concentrated in extracellular viral assemblies (**Fig. 4e**). Tetherin (also known as BST-2 or CD317), is an interferon-inducible transmembrane protein whose degradation by the HIV-1 Vpu protein limits the clustering of HIV-1 virions at the cell surface[34,35]. As the HTLV-1 genome lacks *vpu*-like sequences, tetherin may facilitate virion attachment to the cell surface. Consistent with this, it was previously shown that Vpu expression enhances HTLV-1

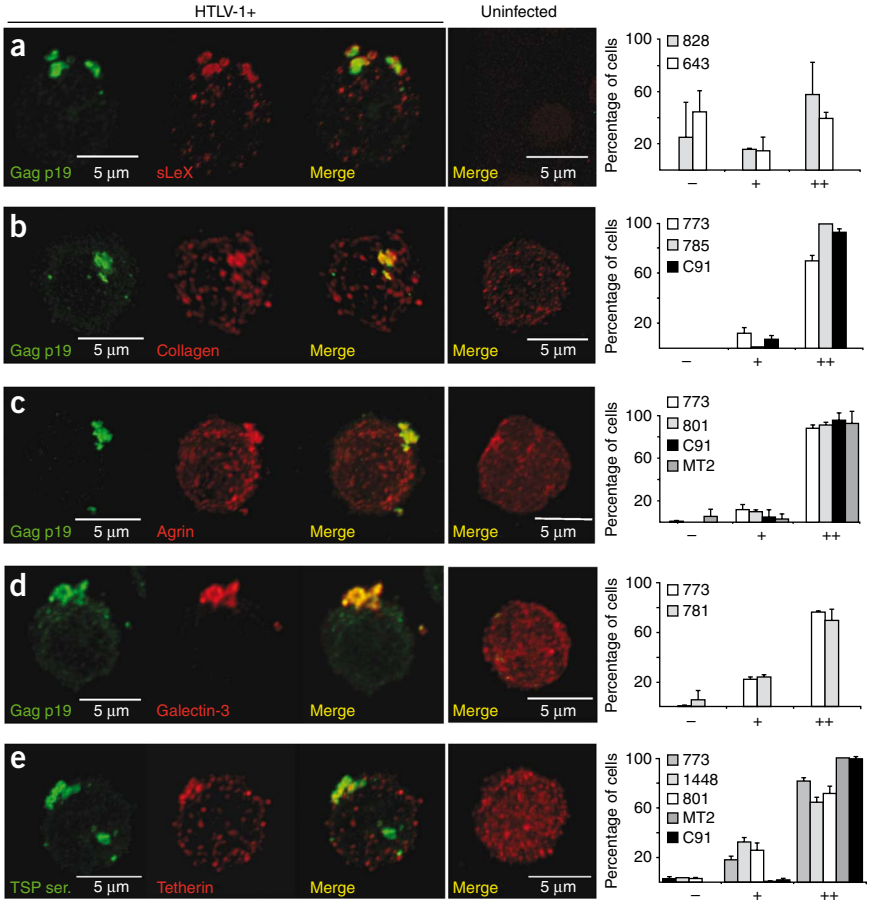

Figure 4 Extracellular matrix and linker proteins are enriched in HTLV-1 viral assemblies. (**a**–**e**) Confocal microscopy of CD4$^+$ T cells from individuals with HAM-TSP immunostained for sialyl-LewisX (sLeX) (red, **a**), for collagen (**b**), agrin (**c**), galectin-3 (**d**) or tetherin (**e**), and for viral proteins (Gag p19 antibody or HAM-TSP serum) (green). Infected (left) and uninfected cells (middle) are shown. Projections of three-dimensional reconstructions are shown. The graphs at right show quantifications of the absence (–), presence (+) or accumulation (++) of each matrix component in cells from several subjects with HAM-TSP (indicated by numbers) and in C91/PL and MT2 cell lines. Data represent means ± s.d. of two independent observer's counts. Data are representative of three experiments for **a**, two for **b** and **d** and five for **c** and **e**.

release[36]. Together, these data support the involvement of extracellular matrix and linker proteins in the cohesion and attachment of HTLV-1 assemblies to the surface of infected cells.

Cell-to-cell transmission of extracellular viral assemblies

Virological synapses have been described as organized cell contacts allowing direct virus transfer through synaptic clefts[4,7]. Consistent with this description, we observed that HTLV-1–infected T cells formed tight cell conjugates and transferred viral proteins to uninfected cells (**Fig. 5**). However, three-dimensional views and vertical *xz* sections of cell conjugates surface-stained with ConA showed extracellular viral assemblies overlapping cell contacts and bridging the gap between both cell surfaces, rather than filling contact sites (**Fig. 5a**). Infected cells were distinguishable from uninfected cells by the presence of cortical viral proteins and significantly ($P < 0.0001$) stronger ConA labeling (**Supplementary Fig. 6a–c** and **Supplementary Fig. 3c**). Conjugates between CD4$^+$ T cells from individuals with HAM-TSP and healthy subjects also showed viral assemblies on the surface of infected and target cells and on the sides of cell contacts (**Fig. 5b**). Extracellular matrix components were transferred together with viral components to target cells (**Supplementary Fig. 6d–f**). We found similar results in MT2-Jurkat cell conjugates; at 10 min, ~35% of conjugates showed Gag p19 labeling on target cells, and this percentage increased until 1 h (**Fig. 5c,d**). The large majority of cell conjugates showed viral assemblies on the sides rather than in the center of the synapse (**Fig. 5c,e**).

Scanning electron microscopy showed Env$^+$ virus clusters very close to cell contact sites (**Fig. 5f**). At 5 min of contact, we had already observed Env$^+$ viral particle clusters on the target cell surface (**Fig. 5g**), indicating that viral assemblies are rapidly transferred to target cells during cell contacts. Finally, transmission electron microscopy revealed Env$^+$ mature viral particles clustered on the sides of cell contacts together with a mesh of electron-dense material, most likely extracellular matrix (**Supplementary Fig. 7a,c**). We also observed Env$^-$ viral particles in potential synaptic clefts (**Supplementary Fig. 7b**), although in a much smaller amount. Thus, during cell contacts, extracellular HTLV-1 assemblies can be rapidly transferred outside the synaptic zone to the surface of other lymphocytes.

Relevance of viral assemblies in HTLV-1 infection

To quantify the relevance of extracellular viral assemblies in HTLV-1 transmission, we removed them by extensive pipetting or by competing the extracellular matrix with heparin that was then removed by several washes. We then measured virus transmission using reporter Jurkat T cells (**Fig. 6a**). The treatments progressively lowered the amount of cell-associated Gag p19, increasing the amount of Gag p19 in cell supernatants (**Fig. 6b,c**). Of note, the capacity of heparin-treated cells to infect reporter cells was strongly diminished (by 80%) and correlated with the amount of cell-associated Gag p19 (**Fig. 6d**). The luciferase activity was due to virus infection, as it was inhibited by the reverse transcriptase inhibitor azidothymidine (**Fig. 6e**). Cell supernatants from washed cells were able to infect reporter target cells, although much less efficiently, provided that they were previously concentrated (**Fig. 6f**). Heparin-containing wash supernatants could compete for virus attachment on target cells (**Fig. 6f**). Mechanical and heparin treatments did not alter the capacity of cells to form cell contacts (**Supplementary Fig. 8**). We obtained similar results when we studied HTLV-1 transmission by T cells from individuals with HAM-TSP (**Fig. 6g**). In conclusion, extracellular viral assemblies account for over 80% of the infectious capacity of HTLV-1–infected cells.

DISCUSSION

We show that HTLV-1–infected cells produce and transiently store virions in extracellular adhesive structures rich in extracellular matrix components and linker proteins that are crucial for HTLV-1 cell-to-cell transmission. Our findings are in line with previously

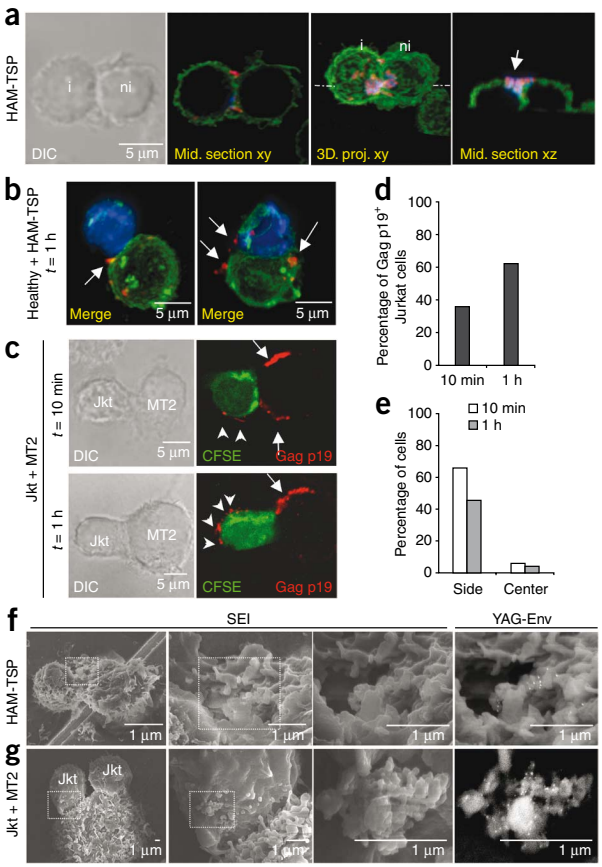

Figure 5 HTLV-1 extracellular viral assemblies spread at cell contacts. (**a**) Confocal microscopy of CD4$^+$ T cell conjugates from individuals with HAM-TSP showing cell surface glycoproteins stained with Con A (green) and viral proteins stained with serum from individuals with HAM-TSP (red) and with Gag p19–specific antibody (blue). Conjugates between infected and uninfected cells were identified by the presence of cortical serum and Gag p19 labeling, and stronger Con A staining of infected cells (i), compared to noninfected cells (ni) (**Supplementary Fig. 6**). Merge images of *xy*-medial optical sections, an *xy* projection of a three-dimensional reconstruction and an *xz*-medial optical section are shown. The arrow points to Gag$^+$TSP Ser$^+$ clusters being transferred from the infected cell to the target cell, bridging the surface of both cells. (**b**) Confocal microscopy of CD4$^+$ T lymphocytes from individuals with HAM-TSP cultured for 1 h with healthy donor CD4$^+$ T lymphocytes labeled with CellTrace Far Red DDAO-SE (blue)[9], stained with ConA (green) and with Gag p19–specific antibody (red). Projections of three-dimensional reconstructions are shown. Arrows point to Gag$^+$ clusters at the cell surface and at the side of the contact. (**c**) Confocal miscroscopy of MT2 cells cocultured with carboxyfluorescein succinimidyl ester (CFSE)-labeled Jurkat cells (Jkt, green) incubated for 10 min or 1 h and then stained with Gag p19–specific mAb. A medial optical section is shown. Gag$^+$ clusters on the surface of the infected cells (arrows) and of target cells (arrowheads) are shown. (**d**) Percentage of Jurkat target cells with Gag$^+$ clusters versus time of coculture. (**e**) Percentage of cell conjugates expressing Gag clustered on the side or in the middle of the synapse versus time of coculture. (**f**) Scanning electron microscopy of T lymphocytes from individuals with HAM-TSP immunogold-labeled for Env gp46. (**g**) Scanning electron microscopy of MT2 cells in contact Jurkat cells (Jkt) for 5 min. The images at right are higher magnifications of the framed areas. SEI and YAG detection reveal cell morphology and gold particles, respectively. Representative of ten experiments performed for **a**, three for **b**, **c** and **f**, five for **g** and two for **d** and **e**.

reported data showing extracellular clusters of HTLV-1 viral particles associated with electron-dense material[37–39]. Extracellular HTLV-1 assemblies are strikingly reminiscent of bacterial biofilms, which are composed of bacteria held together by a carbohydrate-rich extracellular matrix that ensures cohesion, protection, adhesiveness to a substrate and spread upon fragmentation[13]. Bacterial biofilms are rich in exopolysaccharides produced by bacteria[13], but extracellular matrix proteins such as fibrinogen or lectins such as galectin-3 produced by host cells can also cooperate with bacterial proteins, enhancing cohesion and adhesiveness[40–43]. HTLV-1 hijacks similar host cell proteins, enhancing their expression and modifying their carbohydrate composition or their spatial organization to build extracellular assemblies. Notably, whereas collagen, fibronectin, galectin-1 and galectin-3 are overexpressed during HTLV-1 infection[23,24,32,33], we found only collagen and galectin-3 accumulated in viral assemblies, indicating that preferential protein accumulation occurs to build these structures. Moreover, agrin, but not α-dystroglycan, accumulates in viral assemblies, although these two proteoglycans cluster at immunological synapses[26,28]. Finally, HTLV-1 may use host cell adhesion molecules for attachment to the cell surface and for clustering at the uropod.

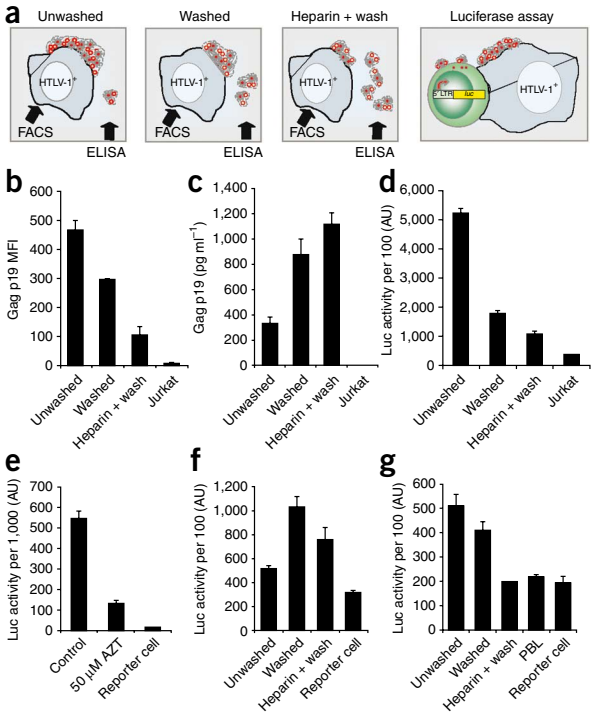

Figure 6 Relevance of extracellular HTLV-1 assemblies for cell-to-cell transmission. C91/PL cells, or primary CD4$^+$ T cells from individuals with HAM-TSP were left unwashed or washed by extensive pipetting, dilution and centrifugation in the absence (washed) or in the presence of heparin (heparin + wash). (**a**) Schematic representation of the experiment. LTR, long-terminal repeat. (**b**) Flow cytometry measurements of Gag p19 that remained associated to C91/PL. (**c**) ELISA measurements of Gag p19 released into the supernatant of C91/PL cells after the various wash treatments. (**d**–**g**) Luciferase activity of reporter Jurkat cells cocultured for 24 h, with C91/PL cells that underwent the various wash treatments (**d**), C91/PL cells in the presence or absence of azidothymidine (AZT) (**e**), 100-fold–concentrated supernatants from C91/PL cells that underwent the various wash treatments (**f**) and HAM-TSP primary CD4$^+$ T cells that underwent the various wash treatments (**g**). Data represent means ± s.d. of triplicates. Representative experiment out of four experiments for **b**–**d**, three for **e** and **f** and two for **g**.

However, the site of virus budding into extracellular viral assemblies, and the contribution of cell-to-cell contacts to the formation or concentration of these structures, remain unknown. Therefore, extracellular matrix components and cellular lectins might together generate cocoon-type structures able to concentrate virions in a confined protective environment. Hyperglycosylation of envelope glycoproteins may help viruses, including HIV-1, to escape immune responses[20,44]. Because HTLV-1 Env glycoprotein is poorly glycosylated, embedding viral particles in carbohydrate-rich supramolecular structures may help HTLV-1 to avoid immune recognition. Moreover, concentrating virions in these structures may locally increase 'infectious titers' and help to convey the virus from cell to cell. Of note, the composition and structure of the extracellular matrix, including collagen and galectin-3, is modified by γ irradiation of cell cultures[45,46]. Therefore, irradiation might reshape the structure of extracellular viral assemblies enhancing viral transmission, explaining why sublethal irradiation of HTLV-1–producing cells increases their efficiency to infect other cells *in vitro*.

As previously reported[4,6,7], we have observed HTLV-1 transmission via cell contacts. However, our data do not support a model of contact-induced virus budding and direct transfer through synaptic clefts, but rather the existence of preformed transient extracellular structures that rapidly adhere to the surface of target cells during cell contacts. Nevertheless, we also observed Env^- viral particles in the synaptic zone, but in a much smaller amount. The functional relevance of extracellular assemblies is supported by the fact that removing these structures strongly inhibits HTLV-1 cell-to-cell transmission. Thus, although heparin washes did not completely remove extracellular viral assemblies, as assessed by fluorescence microscopy, the infectious capacity of cells was markedly reduced. Cell supernatants obtained after cell washes were infectious, although much less efficient than infected cells, indicating that the integrity of extracellular viral assemblies and their transfer at cell contacts are key for HTLV-1 transmission.

Extracellular viral assemblies were resistant to strong shear flow during extensive pipetting, suggesting that they can defy physiological fluid dynamics *in vivo*. Of note, irregular surfaces help the formation and stability of bacterial biofilms. Moreover, some bacteria induce host cell surface reorganization to resist shear flow[47]. Similarly, HTLV-1–infected cells generate numerous ruffles and filopodia that might maintain viral assemblies adhered to the surface of virus-producing cells but also facilitate their transfer to other cells during cell contacts. *In vivo,* viral assemblies might be rapidly transferred to other T lymphocytes or dendritic cells during cell contacts in secondary lymphoid organs. Dendritic cells, in turn, may get infected, again transfer HTLV-1 assemblies to T lymphocytes or both[12]. In addition, dendritic cells might also process viral assemblies and present viral antigens to T lymphocytes, triggering and maintaining the anti–HTLV-1 immune response.

The evolutionary advantage of this transmission mechanism is at present unknown, but it might condition both the virus spread and the immune responses of HTLV-1–infected individuals. It is likely that other viruses have also developed transmission strategies based on similar biofilm-like viral assemblies. As extracellular structures of a particular composition, viral biofilms might be potential targets for future antiviral therapy.

METHODS

Methods and any associated references are available in the online version of the paper at http://www.nature.com/naturemedicine/.

Note: Supplementary information is available on the Nature Medicine website.

ACKNOWLEDGMENTS

This work has been funded by La Ligue Contre le Cancer, l'Association pour la Recherche Contre le Cancer, l'Agence National de Recherche, l'Institut Pasteur PTR-214, and the CNRS. A.-M.P.-C. is supported by Fundação para a Ciência e a Tecnologia, Portugal, V.R. by the European Union Marie Curie Actions Early Stage Training Program Intrapath and R.L. by a Bourse Roux, Institut Pasteur and l'Agence National de Recherche. We thank the US National Institutes of Health AIDS Research and Reference Reagent Program for providing MT2 cells and Env-specific 0.5α antibodies. We thank M. Rüegg (University of Basel) for agrin-specific antibodies, C. Pique (Institut Cochin, Institut National de la Santé et de la Recherche Médicale (INSERM)) for Env gp46–specific antibody and S. Charrin and E. Rubinstein (Institut A. Lwoff, INSERM) for tetraspanin-specific antibodies. We thank S. Ozden and P.-E. Ceccaldi for the C91/PL cell line and expertise, F. Delebecque (Novartis) for the gift of pCS-HTLV-1, and A. Cartaud, J. Cartaud and U. Hazan for sharing expertise. We thank C. Cuche for technical assistance and S. Bassot for technical help with human samples. We thank ICAReB (plateforme d'investigation clinique et d'accès aux ressources biologiques) and the Centre d'Immunologie Humaine, Institut Pasteur for support in biomedical research. We thank, E. Perret, P. Roux, C. Machu A. Danckaert and M.C. Prevost for sharing expertise in microscopy, J.M. Ghigo and S. Wain-Hobson for helpful discussions and R. Mahieux (Ecole Normale Supérieure de Lyon, INSERM) for pLTR-Luc plasmid and for suggestions and critical reading of the manuscript.

AUTHOR CONTRIBUTIONS

A.-M.P.-C. designed and performed experiments. M.S. and S.G. performed electron microscopy experiments. V.R. and R.L. contributed with technical developments for some experiments. O.G. diagnosed and followed subjects with HAM-TSP and provided blood samples. A.G. obtained viroepidemiological data on human samples and collected human cells. A.A. designed the project, designed experiments and wrote the manuscript. M.-I.T. designed the project, designed and performed experiments and wrote the manuscript.

Published online at http://www.nature.com/naturemedicine/.
Reprints and permissions information is available online at http://npg.nature.com/reprintsandpermissions/.

1. Verdonck, K. *et al.* Human T-lymphotropic virus 1: recent knowledge about an ancient infection. *Lancet Infect Dis* **7**, 266–81 (2007).
2. Okochi, K., Sato, H. & Hinuma, Y. A retrospective study on transmission of adult T cell leukemia virus by blood transfusion: seroconversion in recipients. *Vox Sang.* **46**, 245–253 (1984).
3. Donegan, E. *et al.* Transfusion transmission of retroviruses: human T-lymphotropic virus types I and II compared with human immunodeficiency virus type 1. *Transfusion* **34**, 478–483 (1994).
4. Igakura, T. *et al.* Spread of HTLV-1 between lymphocytes by virus-induced polarization of the cytoskeleton. *Science* **299**, 1713–1716 (2003).
5. Barnard, A.L., Igakura, T., Tanaka, Y., Taylor, G.P. & Bangham, C.R. Engagement of specific T-cell surface molecules regulates cytoskeletal polarization in HTLV-1–infected lymphocytes. *Blood* **106**, 988–995 (2005).
6. Nejmeddine, M., Barnard, A.L., Tanaka, Y., Taylor, G.P. & Bangham, C.R.M. Human T-lymphotropic virus type 1 Tax protein triggers micotubule reorientation in the virological synapse. *J. Biol. Chem.* **280**, 29653–29660 (2005).
7. Majorovits, E. *et al.* Human T-lymphotropic virus-1 visualized at the virological synapse by electron tomography. *PLoS One* **3**, e2251 (2008).
8. Jolly, C., Kashefi, K., Hollinshead, M. & Sattentau, Q.J. HIV-1 cell to cell transfer across an Env-induced, actin-dependent synapse. *J. Exp. Med.* **199**, 283–293 (2004).
9. Sol-Foulon, N. *et al.* ZAP-70 kinase regulates HIV cell-to-cell spread and virological synapse formation. *EMBO J.* **26**, 516–526 (2007).
10. Piguet, V. & Sattentau, Q.J. Dangerous liaisons at the virological synapse. *J. Clin. Invest.* **114**, 605–610 (2004).
11. Rudnicka, D. *et al.* Simultaneous cell-to-cell transmission of human immunodeficiency virus to multiple targets through polysynapses. *J. Virol.* **83**, 6234–6246 (2009).
12. Jones, K.S., Petrow-Sadowski, C., Huang, Y.K., Bertolette, D.C. & Ruscetti, F.W. Cell-free HTLV-1 infects dendritic cells leading to transmission and transformation of $CD4^+$ T cells. *Nat. Med.* **14**, 429–436 (2008).
13. Stewart, P.S. & Franklin, M.J. Physiological heterogeneity in biofilms. *Nat. Rev. Microbiol.* **6**, 199–210 (2008).
14. Mazurov, D., Heidecker, G. & Derse, D. HTLV-1 Gag protein associates with CD82 tetraspanin microdomains at the plasma membrane. *Virology* **346**, 194–204 (2006).
15. Jones, K.S., Petrow-Sadowski, C., Bertolette, D.C., Huang, Y. & Ruscetti, F.W. Heparan sulfate proteoglycans mediate attachment and entry of human T-cell leukemia virus type 1 virions into $CD4^+$ T cells. *J. Virol.* **79**, 12692–12702 (2005).
16. Piñon, J.D. *et al.* Human T-cell leukemia virus type 1 envelope glycoprotein gp46 interacts with cell surface heparan sulfate proteoglycans. *J. Virol.* **77**, 9922–9930 (2003).

17. Neu, T.R. & Lawrence, J.R. Lectin-binding analysis in biofilm systems. *Methods Enzymol.* **310**, 145–152 (1999).
18. McClure, S.F., Stoddart, R.W. & McClure, J. A comparative study of lectin binding to cultured chick sternal chondrocytes and intact chick sternum. *Glycoconj. J.* **14**, 365–377 (1997).
19. Le Blanc, I. *et al.* HTLV-1 structural proteins. *Virus Res.* **78**, 5–16 (2001).
20. Coffin, J.M., Hughes, S.H. & Varmus, H.E. *Retroviruses* Ch. 2, 27–70 (Cold Spring Harbor Laboratory Press, 1997).
21. Hiraiwa, N. *et al.* Transactivation of the fucosyltransferase VII gene by human T-cell leukemia virus type 1 Tax through a variant cAMP-responsive element. *Blood* **101**, 3615–3621 (2003).
22. Kambara, C. *et al.* Increased sialyl Lewis^x antigen–positive cells mediated by HTLV-1 infection in peripheral blood CD4$^+$ T lymphocytes in patients with HTLV-1–associated myelopathy. *J. Neuroimmunol.* **125**, 179–184 (2002).
23. Muñoz, E., Suri, D., Amini, S., Khalili, K. & Jimenez, S.A. Stimulation of alpha 1 (I) procollagen gene expression in NIH-3T3 cells by the human T cell leukemia virus type 1 (HTLV-1) Tax gene. *J. Clin. Invest.* **96**, 2413–2420 (1995).
24. Yi, T., Lee, B.H., Park, R.W. & Kim, I.S. Transactivation of fibronectin promoter by HTLV-I Tax through NF-κB pathway. *Biochem. Biophys. Res. Commun.* **276**, 579–586 (2000).
25. Dityatev, A. & Schachner, M. The extracellular matrix and synapses. *Cell Tissue Res.* **326**, 647–654 (2006).
26. Khan, A.A., Bose, C., Yam, L.S., Soloski, M.J. & Rupp, F. Physiological regulation of the immunological synapse by agrin. *Science* **292**, 1681–1686 (2001).
27. Alfsen, A., Yu, H., Magerus-Chatinet, A., Schmitt, A. & Bomsel, M. HIV-1–infected blood mononuclear cells form an integrin- and agrin-dependent viral synapse to induce efficient HIV-1 transcytosis across epithelial cell monolayer. *Mol. Biol. Cell* **16**, 4267–4279 (2005).
28. Zhang, J. *et al.* Agrin is involved in lymphocytes activation that is mediated by α-dystroglycan. *FASEB J.* **20**, 50–58 (2006).
29. Ghez, D. *et al.* Neuropilin-1 is involved in human T-cell lymphotropic virus type 1 entry. *J. Virol.* **80**, 6844–6854 (2006).
30. Tordjman, R. *et al.* A neuronal receptor, neuropilin-1, is essential for the initiation of the primary immune response. *Nat. Immunol.* **3**, 477–482 (2002).
31. Rabinovich, G.A. & Toscano, M.A. Turning 'sweet' on immunity: galectin-glycan interactions in immune tolerance and inflammation. *Nat. Rev. Immunol.* **9**, 338–352 (2009).
32. Hsu, D.K., Hammes, S.R., Kuwabara, I., Greene, W.C. & Liu, F.T. Human T lymphotropic virus-I infection of human T lymphocytes induces expression of the β-galactoside–binding lectin, galectin-3. *Am. J. Pathol.* **148**, 1661–1670 (1996).
33. Gauthier, S. *et al.* Induction of galectin-1 expression by HTLV-I Tax and its impact on HTLV-I infectivity. *Retrovirology* **5**, 105 (2008).
34. Neil, S.J., Zang, T. & Bieniasz, P.D. Tetherin inhibits retrovirus release and is antagonized by HIV-1 Vpu. *Nature* **451**, 425–430 (2008).
35. Van Damme, N. *et al.* The interferon-induced protein BST-2 restricts HIV-1 release and is downregulated from the cell surface by the viral Vpu protein. *Cell Host Microbe* **3**, 245–252 (2008).
36. Jouvenet, N. *et al.* Broad-spectrum inhibition of retroviral and filoviral particle release by tetherin. *J. Virol.* **83**, 1837–1844 (2009).
37. Gessain, A. *et al.* Cell surface phenotype and human T lymphotropic virus type 1 antigen expression in 12 T cell lines derived from peripheral blood and cerebrospinal fluid of West Indian, Guyanese and African patients with tropical spastic paraparesis. *J. Gen. Virol.* **71**, 333–341 (1990).
38. Poiesz, B.J. *et al.* Detection and isolation of type C retrovirus particles from fresh and cultured lymphocytes of a patient with cutaneous T-cell lymphoma. *Proc. Natl. Acad. Sci. USA* **77**, 7415–7419 (1980).
39. Zacharopoulos, V.R., Perotti, M.E. & Phillips, D.M. Lymphocyte-facilitated infection of epithelia by human T-cell lymphotropic virus type I. *J. Virol.* **66**, 4601–4605 (1992).
40. Fowler, M., Thomas, R.J., Atherton, J., Roberts, I.S. & High, N.J. Galectin-3 binds to *Helicobacter pylori* O-antigen: it is upregulated and rapidly secreted by gastric epithelial cells in response to *H. pylori* adhesion. *Cell. Microbiol.* **8**, 44–54 (2006).
41. Moran, A.P. Relevance of fucosylation and Lewis antigen expression in the bacterial gastroduodenal pathogen *Helicobacter pylori*. *Carbohydr. Res.* **343**, 1952–1965 (2008).
42. Gupta, S.K., Masinick, S., Garrett, M. & Hazlett, L.D. *Pseudomonas aeruginosa* lipopolysaccharide binds galectin-3 and other human corneal epithelial proteins. *Infect. Immun.* **65**, 2747–2753 (1997).
43. Bonifait, L., Grignon, L. & Grenier, D. Fibrinogen induces biofilm formation by *Streptococcus suis* and enhances its antibiotic resistance. *Appl. Environ. Microbiol.* **74**, 4969–4972 (2008).
44. Humbert, M. & Dietrich, U. The role of neutralizing antibodies in HIV infection. *AIDS Rev.* **8**, 51–59 (2006).
45. el Nabout, R. *et al.* Collagen synthesis and deposition in cultured fibroblasts from subcutaneous radiation-induced fibrosis. Modification as a function of cell aging. *Matrix* **9**, 411–420 (1989).
46. Joo, H.G. *et al.* Expression and function of galectin-3, a β-galactoside–binding protein in activated T lymphocytes. *J. Leukoc. Biol.* **69**, 555–564 (2001).
47. Mikaty, G. *et al.* Extracellular bacterial pathogen induces host cell surface reorganization to resist shear stress. *PLoS Pathog.* **5**, e1000314 (2009).

ONLINE METHODS

Cell lines and reagents. HTLV-1–infected cell line C91/PL and mAb to HTLV-1 Env gp46 (0.5α) were from the US National Institutes of Health AIDS Research and Reference Reagent Program. The Jurkat cell clone J77cl20 was previously described[48]. Rabbit antibody to agrin (C95) was a gift from M. Rüegg. Mouse Env gp46 4D4–specific antibody[49] was a gift from C. Pique. Mouse mAb to Gag-p19 (TP-7) was from Zeptometrix. We used serum from an individual with HAM-TSP (subject number 1378) with strong reactivity against a panel of viral proteins (HTLV-1 Blot Kit, Genelabs Diagnostics) (A.G., unpublished data). We did not find HTLV-1 protein labeling in cells from healthy donors, in uninfected T cell lines and in a percentage of cells from HTLV-1–infected individuals, supporting the specificity of our antibodies to HTLV-1 proteins (**Figs. 3** and **4**). mAbs to CD15s (CSLEX1) and intercellular adhesion molecule-1 (LB2) were from Becton-Dickinson. Rabbit polyclonal antibody to human collagens I, II, III, IV and V was from AbD Serotec. Mouse mAb to galectin-3 (clone A3A12) was from Affinity BioReagents. Goat antibodies to BST-2 (tetherin) (K-15 and N-17) were from Santa Cruz Biotechnology. Cy3-coupled antibodies to mouse IgG2b, goat IgG, human immunoglobulin and mouse immunoglobulin were from Jackson ImmunoResearch. Fluorescein-coupled mouse IgG1 and IgG2a were from Southern Biotechnology. Alexa^{488}-coupled antibody to fluorescein was from Molecular Probes. Colloidal gold protein A was from the University Medical Center Utrecht. Phycoerythrin-coupled antibody to mouse IgG was from Beckman-Coulter. Metalloproteinases Multipack-1 was from Biomol. Heparinase III was from Sigma. Plant lectins (**Supplementary Fig. 3**) ConA, LCA, *Ulex europeus* (UEAI), *Glycine max* (SBA), *Arachis hypogeae* (PNA), *Triticum vulgaris* (WGA) and *Phaseolus vulgaris* (PHA-E) were from Sigma, and *Hippeastrum hybrid* (HHL) was from Vector Laboratories. CellTrace Far red DDAO-SE (7-hydroxy-9H-(1,3-dichloro-9,9-dimethylacridin-2-one)-succinimidyl ester) was from Invitrogen. HTLV-1 expression plasmid containing the wild-type proviral clone pCS-HTLV-1, allowing the expression of the full-length HTLV-1 genome under the control of the cytomegalovirus immediate early promoter[50], was a kind gift from F. Dellebecque.

Isolation of primary CD4$^+$ T lymphocytes. We purified peripheral blood mononuclear cells through Ficoll-Hypaque centrifugation and isolated CD4$^+$ T cells by negative selection with magnetic cell sorting (Miltenyi Biotec, MACS). We placed the CD4$^+$-enriched T cell population in culture for 18 h as previously described[4,6]. We analyzed cells from seventeen individuals with HAM-TSP and two asymptomatic carriers that contained 2–20% of HTLV-1–infected cells per sample, as assessed by immunofluorescence against viral proteins after 18 h of *ex vivo* culture. We obtained human samples in the context of a Biomedical Research Program approved by the Committee for the Protection of Persons, Ile-de-France III, Tarnier-Cochin, Paris (2007-A01103-50; reference number 2494). All individuals gave informed consent.

Heparinase and metalloproteinase treatments. We treated cells with heparinase III (10 U ml^{-1}) or with a cocktail of metalloproteinases (10 nM) for 1 h at 37 °C in serum-free medium.

Immunofluorescence, confocal microscopy analysis and quantification of fluorescence intensity. We performed immunofluorescence, confocal microscopy analysis and quantification of fluorescence intensity as previously described[48]. We fixed cells with 4% paraformadehyde for 30 min at 25 °C. We performed surface staining (for example, lectin staining) in the absence of detergent. We stained intracellular proteins and Gag p19 after incubating fixed cells in solutions containing 0.05% saponin. Before staining, we blocked non-specific protein binding by incubating the coverslips for 15 min in 5% FCS and 0.05% saponin in PBS. For collagen staining, we treated cells after paraformadehyde fixation with 100% methanol for 40 min at −20 °C. We carried out confocal microscopy analysis on a Zeiss LSM510 using a 63× objective. We acquired Z series of optical sections at 0.2-μm increments. We treated the images by deconvolution using Huygens software to reduce the fluorescence noise of the images. We made three-dimensional image reconstructions of cells and the calculation of the volume of colocalization with Imaris software.

Cell transfection. We isolated peripheral blood CD4$^+$ T cells from healthy donors as described above and then transfected the pCS-HTLV-1 plasmid using Amaxa according to manufacturer. We analyzed transfected cells by fluorescence microscopy after 24 h of culture.

Detachment of extracellular virus assemblies from infected cells. We left HTLV-1–infected cells unwashed or washed them three times in RPMI-1640 serum-free medium and incubated them for 1 h at 37 °C in the absence or in the presence of 50 μg ml^{-1} heparin (Sigma-Aldrich) in serum-free medium. After washing three times in RPMI-1640 with 10% FCS, we processed cells for immunofluorescence analysis and flow cytometry, or to infect luciferase reporter gene target cells. We detected viral antigens on cell culture supernatants by Gag p19 ELISA according to the manufacturer's instructions (Zeptometrix).

Luciferase reporter gene assay. We stably transfected Jurkat cells with a plasmid containing the gene encoding luciferase under the control of HTLV-1 long-terminal repeat (pLTR-Luc). We cocultured luciferase reporter cells in a 96-well round-bottom plate with HTLV-1–infected cells at a cell ratio of 2:1. After 24 h, we assessed luciferase activity using a Promega luciferase kit assay and a TR717 Microplate Luminometer (Berthold Technologies). When indicated (**Fig. 6e**), we incubated reporter cells for 48 h with the reverse transcriptase inhibitor azidothymidine at 50 μM before coculture with HTLV-1–infected cells. We left azidothymidine in the coculture.

Additional methodology. Scanning electron microscopy, transmission electron microscopy and correlative immunofluorescence and transmission electron microscopy are detailed in the **Supplementary Methods** section[51].

48. Thoulouze, M.I. *et al.* Human immunodeficiency virus type-1 infection impairs the formation of the immunological synapse. *Immunity* **24**, 547–561 (2006).
49. Grange, M.P., Rosenberg, A.R., Horal, P. & Desgranges, C. Identification of exposed epitopes on the envelope glycoproteins of human T cell lymphotropic virus type I (HTLV-I). *Int. J. Cancer* **75**, 804–813 (1998).
50. Mahieux, R. *et al.* Extensive editing of a small fraction of human T-cell leukemia virus type 1 genomes by four APOBEC3 cytidine deaminases. *J. Gen. Virol.* **86**, 2489–2494 (2005).
51. Slot, J.W., Geuze, H.J., Gigengack, S., Lienhard, G.E. & James, D.E. Immuno-localization of the insulin regulatable glucose transporter in brown adipose tissue of the rat. *J. Cell Biol.* **113**, 123–135 (1991).

doi:10.1038/nm.2065